

Limit possible electric field in plasmon nanogap resonator

Andrey K. Sarychev,^{*,†} Andrey V. Ivanov,^{*,†} and Grégory Barbillon^{*,‡}

[†]*Institute for Theoretical and Applied Electrodynamics, Russian Academy of
Sciences, 125412, Moscow, Russia*

[‡]*EPF-Ecole d'Ingénieurs, 92330 Sceaux, France*

E-mail: sarychev_andrey@yahoo.com; av.ivanov@physics.msu.ru; gregory.barbillon@epf.fr

Abstract

We propose the theory of the plasmon excited in ultra-narrow plasmonic gap formed by a metal cylinder on a metal surface, that generates a huge resonant local electromagnetic field in optical frequencies. Resonance conditions are found. The maximum possible enhancement of the electric field in the nanogap is estimated as $|E_{max}| / |E_0| \propto |\varepsilon_m|^3 \varepsilon_d^{-1} (\Im \varepsilon_m)^{-2}$. A simple ultranarrow-gaped resonator can be used for SERS sensing and infrared spectroscopy of adsorbed molecules. We assume that a plasmonic nanogap is simplest and most straightforward way to increase flexibility as well as sensitivity of the plasmon-enhanced spectroscopes.

Introduction

Calculation of the electric field in the gap between two metallic cylinders is a classical problem of the classical electrodynamics. However, the metal permittivity is typically negative in optical spectral range, and plasmons are excited between the cylinders, which give a big

enhancement of the local electric field in the crevice.¹ Later, it was shown² that giant optical field fluctuations in random semicontinuous metallic films are due to the local field concentration in-between large metallic clusters. A precise separation of plasmonic nanostructures is of widespread interest, because it controls the build-up of intense and localized optical fields, as well as their spectral tuning.^{3,4} Plasmonic enhancement can also be used to improve the efficiency of photodetectors.⁵ Similarly, the non-linear frequency conversion critically depends on the field enhancements, their spatial localization, and their spectral resonances whose all ultra-sensitivity depends on the plasmonic gaps.⁶ Fundamental processes like quantum tunneling can be observed optically, but only for gap separations in the subnanometer regime.⁷ Graphene could be used as the thinnest spacer between gold nanoparticles and a gold substrate.⁸ The atomic layer deposition of the Al_2O_3 film provides a subnanometer layer that has been employed to successfully fabricate high quality metallic nanogap arrays with sub-5 nm gap size.⁹ In the works,¹⁰⁻¹³ high local electric fields were generated by ultra-narrow gap that formed by gold nanoparticle placed on gold mirror. Evolution of different gap modes with a gap size of 1-5 nm was considered. It was shown that the coupling of transverse and antenna modes is altered by varying the gap size and the nanoparticle shape from sphere to cube, resulting in strongly hybridized modes. Theoretical predictions and experimental studies have shown giant electromagnetic field fluctuations in case of almost touched plasmonic nanoparticles.¹⁴⁻²¹ It was shown that plasmonic nanocavities confining the light to unprecedentedly small volumes, support multiple types of modes. Different nature of these modes leads to mode beating within the nanocavity and the Rabi oscillations, which alters the spatio-temporal dynamics of the hybrid system.¹³ By intermixing plasmonic excitation in nanoparticle arrays with excitons in a WS_2 monolayer inside a resonant metallic microcavity, the hierarchical system was fabricated with the collective microcavity-plasmon-exciton Rabi splitting exceeding 0.5 eV at room temperature. Gap-surface plasmon metasurfaces, which consist of a subwavelength thin dielectric spacer sandwiched between an optically thick film of metal and arrays of metallic subwavelength

elements arranged in a strictly or quasiperiodic fashion, have a possibility to fully control the amplitude, phase, and polarization of the reflected light.²² Such systems are successfully used for surface-enhanced infrared absorption.²³ Strong motivation for the investigation of the gap plasmons is the SERS effect, which relies on the plasmonic enhancement to enable identification of trace molecules captured within gaps. The SERS is extremely important for medical diagnostics, for instance, for cancer detection, imaging and therapy, drug delivery, quantitative control of biomarkers including glycosylated proteins and cardiovascular biomarkers.^{24–28} In recent years, there are many computer simulations as well as experimental works that are devoted to perfect coupled particles with ultra-narrow gaps.^{9,29–34,36–40} In this paper, we propose the theory of the plasmons excited in a ultra-narrow gap formed by a metallic cylinder on a metallic surface for different metals. We find the resonance conditions, when it is possible to achieve possible limit electromagnetic field both inside and in the vicinity of the gap. This will increase the sensitivity of the SERS-probing as well as this of other existing surface enhanced spectroscopes.

Analytical theory

We consider two parallel metallic cylinders whose respective radii are a and $a_1 > a$ that are separated by the distance $d+d_1$ so that the spacing between the cylinder axes is $a+d+a_1+d_1$. The x -axis connects the cylinder centers so the centers have coordinates $\{x, y\} = \{a + d, 0\}$ and $\{-a_1 - d_1, 0\}$, correspondingly, as shown in Fig.1. To find the optical electric field in the nanogap between the cylinders illuminated by the incident light (see Fig.1d), we use new coordinates u and v that convenient to introduce in the complex form $z = L \tanh w/2$, where $z = x + iy$, $w = u + iv$, and the characteristic scale $L = \sqrt{d(2a + d)}$, where d is the distance from the surface of the cylinder “ a ” to the origin of the coordinates. Note a , a_1 , and L fully define the system geometry, if we define $d_1 = \sqrt{a_1^2 + L^2} - a_1 < d$. In the transition from z to w , the whole plane $\{x, y\}$ transforms to the strip $-\infty < u < \infty$, $-\pi < v < \pi$. The surfaces

of the cylinders “ a ” and “ a_1 ” are transformed to the vertical lines $u_d = \ln[(a+d)/(a-d)] > 0$ and $u_{d_1} = -\ln[(a_1+d_1)/(a_1-d_1)] < 0$ (Fig. 1). All the space outer of the cylinders shrinks

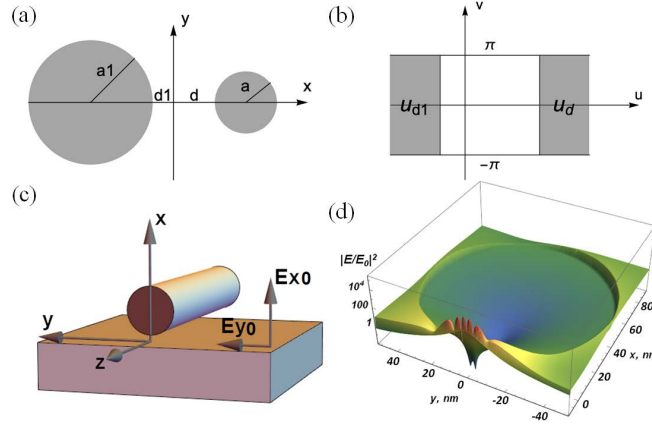


Figure 1: The design of cylindrical nanoparticle-on-mirror cavity. (a-b) Conformal map of two cylinders into $u - v$ strip; (c) metallic cylinder above metal plate, electromagnetic wave is incident from the top; (d) electric field between Ag plate and cylinder with a radius of $a = 50 \text{ nm}$, gap $d = 0.5 \text{ nm}$ calculated at the excitation wavelength of $\lambda = 405 \text{ nm}$.

into the rectangular $[u_{d_1} < u < u_d, -\pi < v < \pi]$. The approach is similar to the map used in.^{16,41} The solution of the Laplace equation in the rectangular can be presented as sum of the functions $f_{Rc}^{(q)} = e^{-qu} \cos qv$, $f_{Rs}^{(q)} = e^{-qu} \sin qv$, $f_{Lc}^{(q)} = e^{qu} \cos qv$, $f_{Ls}^{(q)} = e^{qu} \sin qv$, $q = 1, 2, \dots$:

$$\varphi^G(u, v) = \varphi_0 + \sum_{q=1}^{\infty} \left[A_1^{(q)} f_{Rc}^{(q)} + A_2^{(q)} f_{Rs}^{(q)} + A_3^{(q)} f_{Lc}^{(q)} + A_4^{(q)} f_{Ls}^{(q)} \right] \quad (1)$$

where φ_0 is the potential of the external electric field. We assume that the electric field concentrates in the nanogap whose the size is much smaller than the wavelength of the incident light $d + d_1 \ll \lambda$. Electric potentials in the “ a ” and “ a_1 ” cylinders are given by the following expressions, respectively:

$$\varphi^R(u, v) = \varphi_0 + \sum_{q=1}^{\infty} \left[B_1^{(q)} f_{Rc}^{(q)} + B_2^{(q)} f_{Rs}^{(q)} \right], \quad u > u_d \quad (2)$$

$$\varphi^L(u, v) = \varphi_0 + \sum_{q=1}^{\infty} \left[B_3^{(q)} f_{Lc}^{(q)} + B_4^{(q)} f_{Ls}^{(q)} \right], \quad u < u_{d_1} \quad (3)$$

The components of the electric field in $\{u, v\}$ space $\{E_u, E_v\} = -\nabla_w \varphi = -\{\partial\varphi/\partial u, \partial\varphi/\partial v\}$ are complex since the metal permittivity is complex. Electric field in $\{x, y\}$ space equals to $\{E_x, E_y\} = \hat{J}\{E_u, E_v\}$, where the jacobian \hat{J} is obtained from the derivative $w_z = dw/dz$, namely, $J_{11} = J_{22} = \Re w_z$, $J_{21} = -J_{12} = \Im w_z$. The coefficients $A^{(q)}$ and $B^{(q)}$ in Eqs. (1), (2) and (3) are found from the boundary conditions for the electric fields $E^R = -\nabla_w \varphi^R$, $E^G = -\nabla_w \varphi^G$, and $E^L = -\nabla_w \varphi^L$ at the surface of "a" and "a₁" cylinders:

$$E_v^R = E_v^G, \quad \varepsilon_m E_u^R = \varepsilon_d E_u^G, \quad u = u_d \quad (4)$$

$$E_v^L = E_v^G, \quad \varepsilon_{m_1} E_u^L = \varepsilon_d E_u^G, \quad u = u_{d_1} \quad (5)$$

where ε_m , ε_d , and ε_{m_1} are the permittivities of the "a" cylinder, the outer space, and the "a₁" cylinder, respectively. We expand the external field $E_0 = -\nabla\varphi_0 = \{E_{0x}, E_{0y}\}$ in a series of the functions $f_{Rc}^{(q)}, f_{Rs}^{(q)}, f_{Lc}^{(q)}, f_{Ls}^{(q)}$. For the simplest case of the constant external field, the expansion $\{E_{0u}, E_{0v}\} = \sum_q \{E_{0u}^{(q)}, E_{0v}^{(q)}\}$, has the following form:

$$\{E_{0u}^{(q)}, E_{0v}^{(q)}\} = -2L(-1)^q q \times \begin{cases} E_{0x} f_{Rc}^{(q)} - E_{0y} f_{Rs}^{(q)}, & E_{0x} f_{Rs}^{(q)} + E_{0y} f_{Rc}^{(q)}, & u > 0 \\ E_{0x} f_{Lc}^{(q)} + E_{0y} f_{Ls}^{(q)}, & E_{0y} f_{Lc}^{(q)} - E_{0x} f_{Ls}^{(q)}, & u < 0 \end{cases} \quad (6)$$

where $q = 1, 2, \dots$. We substitute the above equation in the boundary equation (4) for the surface of the "a" cylinder and equate the coefficients at the same $f^{(q)}$ functions obtaining the following equations for the coefficients $\{A^{(q)}, B^{(q)}\}$ in Eqs. (1), (2) and (3):

$$\begin{aligned} \varepsilon_d \left(A_3^{(q)} + A_1^{(q)} g^{2q} \right) - \varepsilon_m B_1^{(q)} &= E_{0x} (\varepsilon_m - \varepsilon_d), \\ \varepsilon_d (A_4^{(q)} - A_2^{(q)} g^{2q}) - \varepsilon_m B_2^{(q)} &= E_{0y} (\varepsilon_m - \varepsilon_d), \\ A_2^{(q)} g^{2q} + A_4^{(q)} - B_2^{(q)} &= A_1^{(q)} g^{2q} - A_3^{(q)} + B_1^{(q)} = 0 \end{aligned} \quad (7)$$

where $g = (L + d)/(L - d)$. Matching electric field and displacement at the surface of the "a₁" cylinder, we obtain from Eq. (5) :

$$\begin{aligned}
\varepsilon_d \left(A_1^{(q)} + A_3^{(q)} g_1^{2q} \right) - \varepsilon_{m_1} B_3^{(q)} &= E_{0x} (\varepsilon_{m_1} - \varepsilon_d), \\
\varepsilon_d \left(A_2^{(q)} - A_4^{(q)} g_1^{2q} \right) - \varepsilon_{m_1} B_4^{(q)} &= E_{0y} (\varepsilon_{m_1} - \varepsilon_d), \\
A_4^{(q)} g_1^{2q} + A_2^{(q)} - B_4^{(q)} &= A_3^{(q)} g_1^{2q} - A_1^{(q)} + B_3^{(q)} = 0 \quad (8)
\end{aligned}$$

where $g_1 = (L + d_1)/(L - d_1)$. Zeroing of the determinant of Eqs.(7) and (8) gives the condition for the “ q ” resonance. The cylinders with the same permittivity $\varepsilon_{m_1} = \varepsilon_m$ resonate when $(gg_1)^{2q} (\varepsilon_d + \varepsilon_m)^2 - (\varepsilon_m - \varepsilon_d)^2 = 0$. The first term dominates when the distance $d + d_1$ between the cylinders increases and $gg_1 \rightarrow \infty$. Then, all the resonance frequencies $\omega_r^{(q)}$ collapse to the single value $\omega_r^{(1)}$ given by the well-known equation $\Re[\varepsilon_d(\omega_r^{(1)}) + \varepsilon_m(\omega_r^{(1)})] = 0$ for the plasmon resonance in a metallic cylinder. On the other hand, when the gap size vanishes $d + d_1 \rightarrow 0$, the factor $gg_1 \rightarrow 1$ from above and the resonance frequencies $\omega_r^{(q)}$ spread out from $\omega_r^{(1)}$ to the minimum resonance frequency estimated from the equation $\varepsilon_m(\omega_r^{(m)}) \simeq -\frac{2\varepsilon_d a a_1}{L(a+a_1)} \rightarrow -\infty$. The real part of the permittivity of the silver, gold, and many other metals is well described by the Drude formula in red and infrared spectral range $\Re\varepsilon_m(\omega) \propto -(\omega_p/\omega)^{2.42}$ and the minimal resonance frequency $\omega_r^{(m)} \propto \omega_p(d/a)^{1/4} \ll \omega_p$.

Observation of the plasmon resonance between metal cylinders is a difficult experimental problem of positioning two nanocylinders parallel each other at a nanosize distance. Yet, the investigation of the plasmon resonance in the metallic nanocylinder placed at nanodistance above a flat metallic surface (i.e., $a_1 = \infty$) is in the center of nowadays experimental studies. To obtain the electric field in the gap between metallic cylinder and metallic surface, we are going to the limit $a_1 \rightarrow \infty$, $d_1 \simeq L^2/2a_1 \rightarrow 0$. The electric field E_0 is fixed at the surface of the large cylinder “ a_1 ” far away from the cylinder “ a ” and all the fields are expressed in terms of this field. After the limit $a_1 \rightarrow \infty$ is taken, the field E_0 is the electric field at the metallic surface $x = 0$, $|y| \gg a$ (see Fig.1c). Thus, we get the electric field in the center coordinates $x = y = 0$, i.e., $u = v = 0$. The electric field $E(x, y)$ has the maximum at this characteristic point just below the cylinder (see Fig.1c,d), the jacobian J reduces to the scalar L , and we obtain by solution of Eqs.(7) and (8) and substitution in Eq.(1):

$$E(0, 0) = \left\{ E_{x0} \left[1 + \frac{8\varepsilon_{m_1}\Sigma}{\varepsilon_d - \varepsilon_m} \right], E_{y0} \left[1 - \frac{8\varepsilon_d\Sigma}{\varepsilon_d - \varepsilon_m} \right] \right\}, \quad (9)$$

$$\Sigma = \sum_{q=1}^{\infty} \frac{(-1)^q q h}{(b+1)^q - h}, h = \frac{(\varepsilon_d - \varepsilon_m)(\varepsilon_d - \varepsilon_{m_1})}{(\varepsilon_d + \varepsilon_m)(\varepsilon_d + \varepsilon_{m_1})}, \quad (10)$$

$$b = (d+L)(2a+d+L)/a^2 \simeq \sqrt{8d/a}, \quad (11)$$

where ε_m , ε_{m_1} and ε_d are the permittivities of the cylinder, metal plate, and outer space. a and d are the cylinder radius and the gap size, respectively. The last approximation in Eq.(11) holds for $d \ll a$. The system resonates if a denominator in Eq.(10) almost vanishes, i.e., the dimensionless parameter $\Re h > 1$ and the loss factor $\kappa = \Im h/|h| \simeq 2\varepsilon_d (\Im \varepsilon_m |\varepsilon_m|^{-2} + \Im \varepsilon_{m_1} |\varepsilon_{m_1}|^{-2}) \ll 1$ for $|\varepsilon_m|, |\varepsilon_{m_1}| \gg \varepsilon_d$.

In spite of simplicity of Eqs.(9) and (10), the gap field has rather rich behavior when the gap vanishes, i.e., $b \rightarrow 0$. Suppose that the parameter $\Re h < 1$, then the denominator $n^{(q)} = (b+1)^q - h$ in the sum Σ in Eq.(10) is not close to zero for all the values of q , and therefore, it can be linearized as $n^{(q)} \simeq b_1 q - h_1$, where $h_1 = h - 1$, $\Re h_1 < 0$, $b_1 = \log(1+b) \simeq b$. Then, Σ approximates as $\Sigma \simeq S(h_1, b_1) = \sum_q^{\infty} (-1)^q q / (b_1 q - h_1)$ and can be solved by Laplace transformation and Abel regularization. The function S has simple integral presentation:

$$\Sigma \simeq S = \frac{h_1(\psi_1 - \psi_2) + b_1}{2b_1^2} = - \int_0^1 \frac{x^{-\frac{h_1}{b_1}} dx}{(x+1)^2 b_1} \quad (12)$$

where $\psi_1 = \psi\left(\frac{b_1-h_1}{2b_1}\right)$, $\psi_2 = \psi\left(-\frac{h_1}{2b_1}\right)$ and $\psi = \Gamma'/\Gamma$ is the polygamma function. The sum approximates as $\Sigma \simeq -\frac{1}{4(b_1-h_1)} \left(\frac{b_1}{2b_1-h_1} + 1\right) \rightarrow \frac{1}{4h_1}$ for the fixed h_1 and $|b_1/h_1| \rightarrow 0$. That is the electric field tends towards a finite value when the gap between cylinder and plate vanishes. The integral (12) converges for $\Re h_1/b_1 < 1$. In the opposite case, one of the denominators $n^{(q)}$ in the sum Σ in Eq.(10) vanishes for $q = q_c = \log h / \log(1+b)$. We linearize the denominator at this point obtaining $n^{(q)} \simeq [dn^{(q)}/dq](q - q_c) = qb_2 - h_2$, where $b_2 = h \log(1+b)$ and $h_2 = h \log h$. The terms in Σ with numbers close to $q_1 = \Re q_c$ make

maximum impact to the sum Σ . The analytical continuation of the function $S(b_2, h_2)$ to the domain $\Re[h_2/b_2] < 0$ gives :

$$\Sigma \simeq -\frac{x^2}{b_2 \sin(x)} - S(-h_2, b_2) \quad (13)$$

where $x = \pi h_2/b_2 = \frac{\pi \log h}{\log(1+b)} \simeq \frac{\pi \log |h|}{\log(1+b)} + i \frac{\pi \kappa}{\log(1+b)}$. The first resonance term in Eq. (13) determines the singular behavior of the field when the loss factor $\kappa \ll 1$. Suppose that the frequency is fixed, then the sum $|\Sigma|$ oscillates as function of $b \ll \log |h|$ (see Fig. 2).

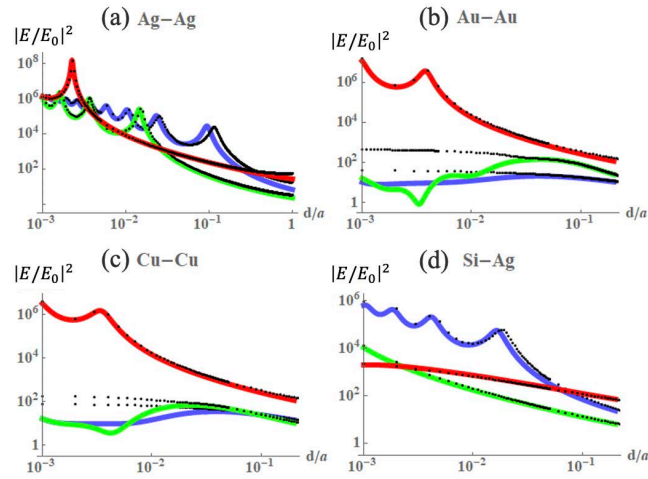


Figure 2: Comparison of analytical (lines) and numerical (dots) electric field intensities $|E/E_0|^2$ in the gap between (a) Ag cylinder and Ag surface, (b) Au cylinder and Au surface, (c) Cu cylinder and Cu surface, (d) Si cylinder and Ag surface. Red, green and blue lines correspond to the excitation wavelengths of 785 nm/532 nm/405 nm, respectively. The excitation beam has an incidence angle of 45° , and a p -polarization. The results are shown in logarithmic scale.

The oscillation period decreases with decreasing of the gap size. The local maxima $|\Sigma|_m$ are achieved when $\Re x = m\pi$. The value of these maxima is given by the following expression:

$$|\Sigma|_m \simeq \frac{\pi m^2}{|h_2|} \sinh \left(\frac{\pi m \kappa}{\log |h|} \right)^{-1} \quad (14)$$

This value linearly increases with the number m : $|\Sigma|_m \propto m/\kappa$ achieving absolute maximum for $m = m_{mx} \simeq \log |h|/\pi\kappa$, namely, $|\Sigma|_{mx} \simeq \log |h|/(\pi\kappa^2|h|)$. The oscillations collapse with further decrease the gap due to the losses in the system and $|\Sigma|$ exponentially drops down

as function of b . Substituting $|\Sigma|_{mx}$ in Eq. (9), we obtain the estimation of the limit of the electric field

$$|E_{mx}|^2 \simeq \frac{64 |h|^4 \log^2 |h|}{\pi^2 (\Im h)^4} |E_{00}|^2 \quad (15)$$

where $|E_{00}|^2 = |E_{0x}\varepsilon_{m1}|^2 + |E_{0y}\varepsilon_d|^2$, ε_m , ε_{m1} and ε_d are the permittivities of the metallic cylinder, metallic plate and surrounding space, respectively. In the red and infrared spectral ranges, the metal permittivity is large in absolute value ($|\varepsilon_m|, |\varepsilon_{m1}| \gg \varepsilon_d, \Im\varepsilon_m/|\varepsilon_m|, \Im\varepsilon_{m1}/|\varepsilon_{m1}| \ll 1$) and Eq. (15) simplifies:

$$|E_{mx}^2| \propto \frac{|\varepsilon_m^6| |\varepsilon_{m1}^4| (|\varepsilon_m| + |\varepsilon_{m1}|)^2}{\varepsilon_d^2 (|\varepsilon_m^2| \Im\varepsilon_{m1} + |\varepsilon_{m1}^2| \Im\varepsilon_m)^4} |E_{00}|^2 \quad (16)$$

The maximum field enhancement estimates as $|E_{mx}| \propto |\varepsilon_m|^3 \varepsilon_d^{-1} (\Im\varepsilon_m)^{-2} |E_0|$ in the gap between cylinder and plate made of the same metal. For instance, the field could be as large as $|E_{mx}| > 10^3 |E_0|$ in the gap between the silver plate and a silver cylinder for the green light $\lambda = 532 \text{ nm}$ (Fig. 2a). It is an upper limit since the field could be restricted by radiation loss and the spatial dispersion of the electric charge in subnanometer gap.³

Analytical theory vs. Simulations

In any real experiment, a layer of investigated molecule is placed in the gaps formed by metallic particles distributed over a metallic mirror. We use full-scale computer simulations in COMSOL environment to simulate the periodic array of metallic nanocylinders with the radius $a = 10 \text{ nm}$, period of $D = 200 \text{ nm}$, and for "large" metallic nanocylinders, $a = 50 \text{ nm}$ and $D = 200 \text{ nm}$. The cylinders are placed over the metal surface and are excited by p -polarized light with an incidence angle of 45° similar to.¹⁰ The periodic boundary conditions and periodic ports are used to compute the reflectance as well as local electric field. Thus obtained, the enhancement of the gap electric field is in agreement with analytical theory as shown in Figs.2 a-c. The gap field could also achieve large values in the metal-semiconductor

(dielectric) gap (Fig.2d). The field enhancement in the gap between a cylinder and the

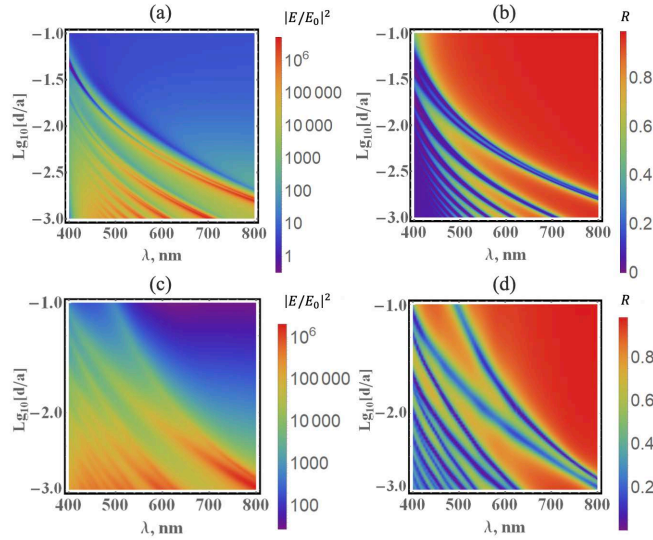


Figure 3: Analytical results in the gap between Ag cylinder and Ag surface as function of wavelength and d/a ratio: (a) electric field intensity $|E/E_0|^2$ and (b) reflectance. Numerical results for “large” silver cylinder with a radius of $a = 50 \text{ nm}$ and a period of $D = 200 \text{ nm}$: (c) electric field intensity $|E/E_0|^2$ and (d) reflectance.

surface could revile itself in the anomalous reflectance (Fig. 3 b,d).

To compare the theory with computer simulations, we fix the electric field E_s at the point $x = d + 2a, y = 0$ on the surface of a cylinder and calculate the field $E(x, y)$ in all the space by using our analytical theory. To simplify the consideration, the direct interaction between cylinders is neglected since the electric field is localized in the nanogaps with size $d \ll a$. Then, we average the field over the layer $0 < x < d + 2a$ and introduce the effective permittivities $\varepsilon_{xx}^{(e)} = \langle \varepsilon(x, y) E_x(x, y) \rangle / \langle E_x(x, y) \rangle$ and $\varepsilon_{yy}^{(e)} = \langle \varepsilon(x, y) E_y(x, y) \rangle / \langle E_y(x, y) \rangle$. Electromagnetic wave with an amplitude E_{in} and the p -polarization is incident on the layer placed above the metal plate. Maxwell equations are solved in terms of the amplitude E_{in} in order to find electromagnetic field in the layer with thickness $d + 2a$ and permittivity $\hat{\varepsilon}^{(e)}$. In particular, we find the electric field $E_0 = \{E_{x0}, E_{y0}\}$ at the interface between the layer and the metal plate (see Fig. 1c). In the dilute case $a \ll D \ll \lambda$, the field E_0 equals to the field that were on the metal surface without cylinder, namely

$E_0 = E_{in} \left\{ \frac{\varepsilon_{m_1} \sin 2\theta}{\sqrt{\varepsilon_d \varepsilon_{m_1} - \varepsilon_d^2 \sin^2 \theta + \varepsilon_{m_1} \cos \theta}}, \frac{2 \cos \theta \sqrt{\varepsilon_d \varepsilon_{m_1} - \varepsilon_d^2 \sin^2 \theta}}{\sqrt{\varepsilon_d \varepsilon_{m_1} - \varepsilon_d^2 \sin^2 \theta + \varepsilon_{m_1} \cos \theta}} \right\}$, where θ is the angle of the incidence. This field is introduced in Eq.(9) in order to obtain the analytical esteem of the electric field in the nanogap. The theoretical results are in accordance with full-scale computer simulations for small cylinders ($ka \ll 1$). The results of our quasistatic theory being extrapolated to $ka \sim 1$ are still in a qualitative agreement with computer simulations of "large" nanocylinders (Fig.3). The agreement is better for the smaller gap size d and higher plasmon resonance q . The theory holds when the plasmon size $L_q \sim \sqrt{ad}/q$ is smaller than the skin depth $L_q \ll \frac{1}{k\sqrt{|\varepsilon_m|}}$. Figures 2 and 3 show that the largest field enhancement is achieved in red and infrared spectral bands, where optical loss in metal is relatively small. On the other hand, the silver-silicon system resonates for $\lambda < 550 \text{ nm}$ when the parameter $\Re h$ in Eq.(10) becomes larger than one.

In summary, we present a theory of the plasmons excited in the gap between a metal or dielectric nanocylinder and a metallic or dielectric plate. The resonance conditions for the gap plasmon are found as function of the metal permittivity and the gap size. When the cylinder-on-mirror cavity is excited by the incident light, the gap electric field increases and oscillates with decreasing the gap size achieving its limit value. Excitation of the gap plasmons results in the dips in the reflectance. The " q -th" minimum of the reflectance corresponds to the excitation of the " q -th" order plasmon. Fluctuations in the reflectance were probably observed, e.g., in experiments.^{3,35} The quasistatic theory qualitatively describes the field enhancement up to $ka \leq 1$, since the field concentrates in the nanogap whose size is much smaller than λ . Finally, this analytical theory can be used to design new SERS substrates and other optical sensors.

The work is supported by Russia Fund Basic Research grant 20-21-00080.

References

- (1) F. J. Garcia-Vidal, and J. Pendry, Phys. Rev. Lett. **77**, 1163 (1996).

- (2) S. Grésillon *et al.*, Phys. Rev. Lett. **82**, 4520 (1999).
- (3) C. Ciraci *et al.*, Science **337**, 1072 (2012).
- (4) A. Moreau *et al.*, Nature **492**, 86 (2012).
- (5) T. J. Echtermeyer *et al.*, Nat. Commun. **2**, 458 (2011).
- (6) Y. Zhang *et al.*, Nano Lett. **11**, 5519 (2011).
- (7) K. J. Savage *et al.*, Nature **491**, 574 (2012).
- (8) J. Mertens *et al.*, Nano Lett. **13**, 5033 (2013).
- (9) H. Cai *et al.*, Opt. Express **24**, 20808 (2016).
- (10) S. Mubeen *et al.*, Nano Lett. **12**, 2088 (2012)
- (11) R. Chikkaraddy *et al.*, ACS Photonics **4**, 4649 (2017).
- (12) R. Chikkaraddy *et al.*, Nano Lett. **18**, 405 (2018).
- (13) A. Demetriadou *et al.*, ACS Photonics **4**, 2410 (2017).
- (14) K. Seal *et al.*, Phys. Rev. Lett. **94**, 226101 (2005).
- (15) D. Genov, *et al.*, Nano Lett. **4**, 153 (2004).
- (16) A. Ivanov *et al.*, Appl. Phys. A **107**, 17 (2012).
- (17) L. L. Frumin, A. V. Nemykin, S. V. Perminov, and D. A. Shapiro, J. Opt. **30**, 2048 (2013).
- (18) Z.-q. Liu *et al.*, Plasmonics **8**, 1285 (2013).
- (19) G.-q. Liu *et al.*, Phys. Chem. Chem. Phys. **16**, 4320 (2014).
- (20) G.-q. Liu *et al.*, Opt. Commun. **316**, 111 (2014).

- (21) I. L. Rasskazov, V. A. Markel, and S. V. Karpov, *Opt. Spectrosc.* **115**, 666 (2013).
- (22) F. Ding, Y. Yang, R. A. Deshpande, and S. I. Bozhevolnyi, *Nanophotonics* **7**, 1129 (2018).
- (23) L. Dong *et al.*, *Nano Lett.* **17**, 5768 (2017).
- (24) J. Kneipp, *ACS Nano* **11**, 1136 (2017).
- (25) Y. Hu *et al.*, *ACS Nano* **11**, 5558 (2017).
- (26) C. Andreou *et al.*, *ACS Nano* **10**, 5015 (2016).
- (27) N. L. Nechaeva *et al.*, *Anal. Chim. Acta* **1100**, 2506 (2020).
- (28) H. Chon *et al.*, *Chem. Commun.* **50**, 1058 (2014).
- (29) Q. Fu *et al.*, *ACS Appl. Mater. Interfaces* **7**, 13322 (2015).
- (30) T. Jiang *et al.*, *J. Am. Chem. Soc.* **140**, 15560 (2018).
- (31) G. Liu *et al.*, *Sol. Energy Mater. Sol. Cells* **186**, 142 (2018).
- (32) X. Lu *et al.*, *Chem. Mater.* **30**, 1989 (2018).
- (33) C. Ma, Q. Gao, W. Hong, J. Fan, and J. Fang, *Adv. Funct. Mater.* **27**, 1 (2016).
- (34) J.-M. Nam, J.-W. Oh, H. Lee, and Y. D. Suh, *Acc. Chem. Res.* **49**, 2746 (2016).
- (35) K.N. Kanipe et al. *J. Phys. Chem. C* **121** 14269 (2017)
- (36) R. Pan *et al.*, *Nanoscale* **10**, 3171 (2018).
- (37) Y. Shin, J. Song, D. Kim, and T. Kang, *Adv. Mater.* **27**, 4344 (2015).
- (38) D. O. Sigle *et al.*, *ACS Nano* **9**, 825 (2015).
- (39) D. Yoo *et al.*, *Nano Lett.* **18**, 1930 (2018).

(40) J. Zhou *et al.*, ACS Nano **10**, 11066 (2016).

(41) M. Kraft *et al.*, Phys. Rev. X **5**, 031029 (2015).

(42) P. B. Johnson, and R. W. Christy, Phys. Rev. B **6**, 4370 (1972).